Amphiphilic Networks. XI. Mechanical Properties and Morphology

DONGKYU PARK,* BALAZS KESZLER, VASSILIOS GALIATSATOS, JOSEPH P. KENNEDY

Maurice Morton Institute of Polymer Science, The University of Akron, Akron, Ohio 44325-3909

ABSTRACT: The bulk properties of two types of amphiphilic networks, poly(2-hydroxyethyl methacrylate)-*l*-polyisobutylene (PHEMA-*l*-PIB, H-network) and poly(*N,N*-dimethylacrylamide)-*l*-polyisobutylene (PDMAAm-*l*-PIB, A-network), have been investigated. Tensile strengths decreased considerably by swelling, and the decrease was more severe by swelling in water than in *n*-heptane. Elongations increased by swelling in water; however, the change was not consistent upon swelling in *n*-heptane. The hardness of dry networks decreased with increasing PIB content, while for wet networks it was similar to dry networks containing 85 wt % PIB. Small-angle X-ray scattering showed that average interdomain spacings decreased with increasing PIB content. According to dynamic mechanical thermal analysis (DMTA) the glass transition temperatures (T_g) of the respective hydrophobic and hydrophilic components shift toward each other with increasing PIB content. A "liquid–liquid transition" (T_{ll}) above the T_g of the hydrophilic component was apparent by DMTA, but could not be found by differential scanning calorimetry (DSC). © 1997 John Wiley & Sons, Inc. J Appl Polym Sci **66**: 901–910, 1997

Key words: amphiphilic networks; mechanical properties; morphology; transition

INTRODUCTION

Amphiphilic networks consisting of two incompatible polymers, one hydrophilic and one hydrophobic, linked together in a random two-component network system were recently developed by Kennedy and coworkers.[1–5] These materials become soft and rubbery upon hydration and resemble the consistency of living tissues. Swelling and drug release kinetics suggest potential applications as controlled drug delivery devices.[6] Amphiphilic networks with 50 : 50 wt % hydrophilic/hydrophobic contents were found to exhibit excellent biocompatibility and hemocompatibility *in vivo*[7] and *in vitro*.[8]

Very recently, the surface chemistry,[9,10] morphology,[9,10] and energetics[10,11] of H- and A-networks were investigated by X-ray photoelectron spectroscopy, atomic force microscopy, and dynamic contact angle measurements. For biomedical applications, bulk properties as well as surface properties are important. If a biomedical material is to be used as an implant, its mechanical properties must be evaluated. For example, a mismatch in compliance between noncompliant vascular prostheses and the artery is reported to cause trauma to the arterial wall and stimulates thrombosis and initial hypertrophy.[12] Bulk morphology is also of importance in regard to blood compatibility because domain sizes and shapes in the bulk are similar to those on the surface. Hydrophilic–hydrophobic microphase-separated structures, as in normal vascular endothelium, show good antithrombogenicity.[13–17]

This article is concerned with tensile properties, hardness, average interdomain spacing, mor-

phology, and dynamic mechanical properties of dry and swollen amphiphilic networks. The effects of water- and n-heptane-swelling on tensile properties and morphology were investigated by tensile measurements and small-angle X-ray scattering (SAXS), respectively. The morphology of the networks was studied in relation to T_g and $T_{ll}(>T_g)$ obtained by dynamic mechanical thermal analysis (DMTA) and differential scanning calorimetry (DSC). Thermal degradation of the networks was investigated by thermogravimetric analysis (TGA).

EXPERIMENTAL

Materials

The amphiphilic networks were synthesized by simultaneous copolymerization/crosslinking of acrylate or methacrylate monomers with polyisobutylene end-capped with methacrylate (MA-PIB-MA) using tetrahydrofuran (THF) as common solvent.[2–5] Crosslinked polyisobutylene (PIB) was synthesized by free radical-induced polymerization of MA-PIB-MA, and cross-linked poly-(2-hydroxyethyl methacrylate) (PHEMA) and poly(N,N-dimethylacrylamide) (PDMAAm) by copolymerization of 2-hydroxyethyl methacrylate (HEMA) and N,N-dimethylacrylamide DMAAm with 5 mol % of ethylene glycol dimethacrylate, respectively. The synthesis conditions were described earlier.[2–5] The number average molecular weight ($\bar{M}_n$) of PIB was 3800, 4300, 4500, 10,000, and 15,000 g/mol, with dispersies < 1.10. Unswollen samples were dried in a vacuum oven at ~ 110°C for a week and stored in a desiccator until measurement. The symbolism to designate the samples was introduced and its use is consistent with the earlier articles of this series[2–10]; for example, in the symbol H-4.5-35, H stands for H-network, the first number (4.5) is the $\bar{M}_n$ of PIB in thousands, and the second number (35) is the weight percent of PIB in the network. Swollen samples were prepared by placing the networks in distilled water or n-heptane (reagent grade) at 23 ± 3°C for at least 3 days to reach equilibrium swelling.

Tensile Tests

Tensile properties were obtained on an Instron instrument (Instron Universal Test Instruments, Table Model) with a 5 or 50 kg load cell and 5 cm/ min crosshead speed at room temperature with microdumbbells. The microdumbbells (3.1 mm gauge width and 12 mm gauge length) were cut from dry 0.23–0.55-mm-thick sheets. Swollen specimens were prepared by swelling dry microdumbbells; thus their volumes increased depending on the extent of equilibrium swelling.[5] To minimize the effect of drying on swollen samples during size measurements, the samples were frequently wetted with the swelling solvent before stretching. Averages of five measurements are reported.

Hardness Measurements

Test specimens were at least 6 mm thick. Averages of five measurements for dry and wet (equilibrated in water) samples are reported. A Type A durometer was used for soft materials (i.e., wet samples and dry samples with > 70 wt % PIB), and a type D for harder materials (i.e., other dry samples).

Small-Angle X-Ray Scattering (SAXS)

Average long spacing was measured by using Rigaku Denki small angle X-ray scattering equipment. The X-ray source was obtained by Rigaku Denki Rotaflex RU-200 D/max rB 12 kW generator. A Ni filter was used to achieve a CuK_α monochromatic radiation corresponding to a wavelength of 0.1542 nm. Desirable scattering intensity was obtained within 20 min. Lorentz corrections of a SAXS curve were done by multiplying the intensity (I) by s^2 ($s = 2 \sin \theta/\lambda$), where s is the scattering vector, θ Bragg's angle, and λ the wavelength of scattered radiation. The average interdomain spacing was obtained by a one-dimensional collinear correlation function, $\gamma(x)$.[18] A plot of correlation function versus correlation distance was obtained by curve-fitting the Lorentz-corrected SAXS curves. The flat SAXS specimen was 1.0–2.0 mm thick and 5×5 mm^2 wide. n-Heptane-swollen samples were wrapped with aluminum foil to prevent solvent evaporation during measurement.

Thermogravimetric Analysis (TGA)

Thermal degradation temperature was obtained by a Du Pont 951 thermogravimetric analyzer coupled with a Du Pont 9900 computer/thermal analyzer in air with 10°C/min heating rate.
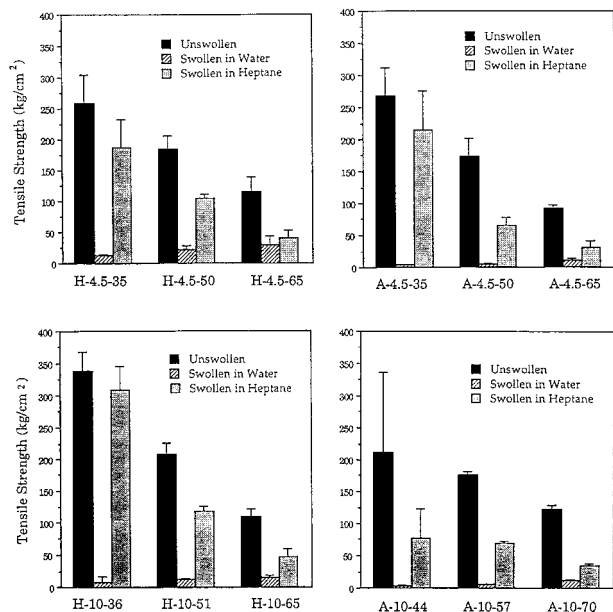
Figure 1 Tensile strength of dry and swollen amphiphilic networks.

Dynamic Mechanical Thermal Analysis (DMTA)

DMTA was carried out by a dynamic mechanical thermal analyzer (Polymer Laboratory, Inc., England) with shear mode and small clamps/small studs at 4°C/min heating rate, 32-μm strain, and 1-Hz frequency, using 0.5–2.1-mm-thick disk-shaped samples of 5.0–7.5-mm diameter.

Differential Scanning Calorimetry (DSC)

Thermal analysis was done by a Du Pont 910 differential scanning calorimeter coupled with a Du Pont 9900 computer/thermal analyzer with 10°C/min heating. To minimize noise of the DSC trace, the weight of the encapsulated sample was 15–20 mg. To obtain data with the same thermal history, the encapsulated sample was first heated at 150°C for 5 min in a DSC cell, quenched to -120°C or lower (together with the DSC cell) with liquid nitrogen, and then DSC was run immediately.

RESULTS AND DISCUSSION

Tensile Properties

Tensile tests were performed on both dry and water- or n-heptane-swollen H- and A-networks. Figures 1 and 2, respectively, show tensile strengths and elongations of dry and swollen net-

works. As expected, tensile strength decreased, whereas elongation increased with increasing PIB content in the dry networks. Tensile properties of H- and A-networks having different $\bar{M}_n$ of PIB were not markedly different.

In general, the tensile strength of networks decreases by swelling because the number of chains per unit volume decreases by the solvent in the network. The greater the extent of swelling, the greater the decrease in tensile strength. The tensile strength of the A-networks decreased more by water-swelling than those of H-networks. This is because the former are more hydrophilic and thus swell more than the latter. However, the extent of the decrease was not the same even though the extent of swelling by different solvents was the same; the decrease was much stronger for water-swollen samples than for n-heptane-swollen samples. This is exemplified by H-4.5-50, the swelling ratio of which is similar in water and in n-heptane. Thus, with amphiphilic networks, as in the case of general polymer networks, the decrease in tensile strength depends not only on the extent of swelling but also on the nature of the swelling solvent. This is probably due to specific solvent effects,[19] which are prominent at lower values of the volume fraction of polymer. These effects are thought to originate from solvent-induced changes in conformational energy, and thus in configuration and size, of the chains. These ef-
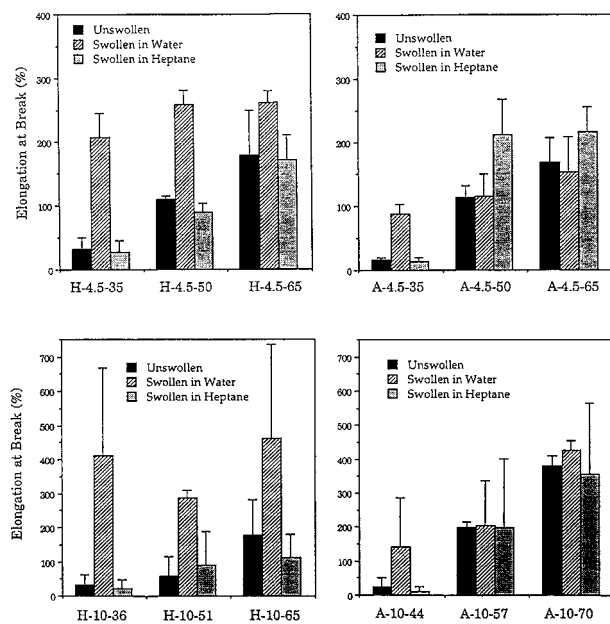

Figure 2 Elongation of dry and swollen amphiphilic networks.

fects do not correlate with the cohesive energy density or the dielectric constant of the solvent.[19]

An alternative explanation is as follows. In the dry state the hydrophilic chains are glassy, and thus stiffer than the hydrophobic PIB chains. When the amphiphilic network is swollen in water, which act as a plasticizer and transforms the glass into a rubber, the strength of the swollen hydrophilic chains will decrease, which reduces the strength of the networks. In contrast, when the amphiphilic network is swollen in n-heptane, the strength of the swollen hydrophobic chains will decrease much less than with water-swollen hydrophilic chains, and the mechanical properties of the soft PIB rubber will not change significantly by swelling.

The effect of swelling on elongation could be explained similarly. By swelling in water, the elongation of H-networks increases considerably, since the glassy hydrophilic chains become soft and flexible by absorbing water. However, the A-networks did not show a consistent trend: in some compositions the elongation did not increase much by swelling in water, probably because these networks swell excessively in water,[#] and hence form too weak and loose networks to have high elongations. Swelling in n-heptane of both H- and A-networks did not result in significant elongation change, most likely for the same reason as proposed above for the tensile strengths.

Hardness

The hardness of dry and wet networks was obtained from durometer readings. Since the values obtained from a Type A durometer cannot be compared directly with those from a Type D durometer, the readings were converted to force (in N) by

$$N = 0.550 + 0.075H_A$$

where H_A is the hardness by a Type A durometer, and

$$N = 0.4445H_D$$

where H_D is the hardness by a Type D durome-

[#] The equilibrium swelling ratio by weight [= solvent (g)/ network (g)] in water was 1.4, 0.95, 0.63, and 0.36 for A-4-26, A-4-45, A-4-56, and A-4-59, respectively, while it was 0.27, 0.21, 0.16, and 0.10 for H-4-29, H-4-37, H-4-49, and H-4-57, respectively. For details, see ref. 5.
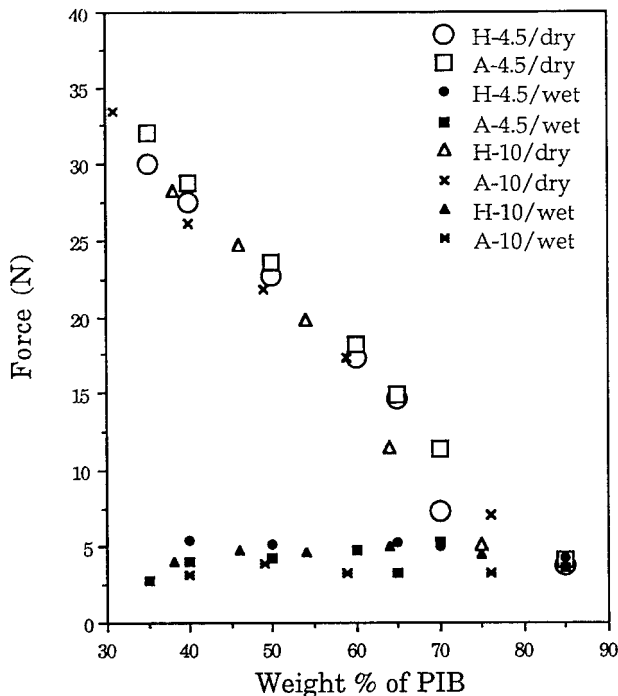
Figure 3 Hardness (converted in force) of amphiphilic networks for dry and swollen networks.

ter.[20] Figure 3 shows N, i.e., the applied force to the intendor during penetration into the network against the wt % of PIB in the networks. The hardness of the dry networks decreased with increasing PIB content in both series, while the hardness of wet networks was similar to the dry networks containing 85 wt % PIB, regardless of composition. Networks with higher molecular weight PIB showed somewhat lower hardness, which suggests looser structures.

Morphology

According to transmission electron microscopy,[5] networks H-4-49 and H-9.5-56 are co-continuous and the PHEMA phase forms $\sim$ 10 Å-diameter interconnecting channels. Large PHEMA islands of $\sim$ 100 Å diameter may also be present, most likely due to aggregated dangling PHEMA chain-ends.

Morphological information in terms of the magnitude and periodicity of electron distribution could be obtained from the angular dependence of scattered SAXS intensity.[18] Average interdomain spacings (i.e., interdomain distances or long spacings) were determined by the position of the maxima on Lorentz-corrected SAXS curves for dry and swollen networks, and the results are shown in

Table I Average Interdomain Spacings of Dry and Swollen Networks

| Sample	M_c[a] of Hydrophilic Polymer (g/mol)	Average Interdomain Spacing (Å)		
		Dry	in Heptane	in Water
H-4.3-15	12,183	173	—	—
H-4.3-35	3,993	126	126	127
H-4.3-50	2,150	117	121	119
H-4.3-65	1,158	99	120	100
H-4.3-85	379	74	—	—
A-4.3-35	3,993	112	113	—
A-4.3-50	2,150	108	119	—
A-4.3-65	1,158	84	109	—
A-4.3-85	379	62	—	—

Values determined by the position of the maxima on Lorentz-corrected SAXS curves.

[a] Number avrage molecular weight between crosslink points (M_c) was calculated from $M_c = (W_h \bar{M}_n)/2W_{PIB}$, where W_h and W_{PIB} are the weight fraction of the hydrophilic polymer and PIB, respectively, and $\bar{M}_n$ is the number average molecular weight of the MA-PIB-MA.

Table I. Figures 4 and 5 show the plots of the correlation function $[\gamma(x)]$ versus correlation distance (x) for H- and A-networks, respectively. $\gamma(x)$ is a probability function and represents a measure of the extent of inhomogeneity in electron density distribution.[18] The small value of interdomain spacing indicates microphase-separated structures. Average interdomain spacings in both H- and A-networks decrease with increasing PIB concentration because the PIB crosslinker suppresses phase separation of the two incompatible components. At the same PIB content, the average interdomain spacings of A-networks were smaller than those of H-networks, indicating that

the A-networks are more homogeneous than the H-networks.

The values for water-swollen A-networks could not be obtained because of insufficient electron density difference between PIB and water-swollen hydrophilic domains. Swelling in n-heptane or water increases the interdomain spacing for almost all networks in proportion to the extent of swelling. However, the effects of n-heptane and water on the interdomain spacing of H-networks were different. Water-swollen H-4.3-50 showed lower interdomain spacing values than heptane-swollen H-4.3-50 even though the extent of swelling (by weight) in water and heptane was similar.[5] This phenomenon is more distinct upon com-
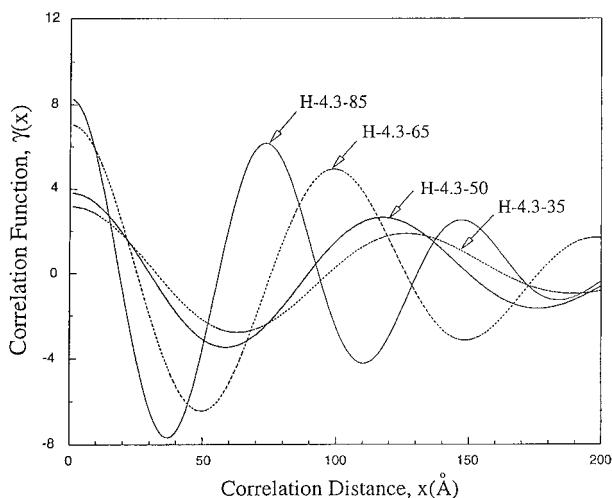
Figure 4 Correlation functions obtained from SAXS measurements for H-networks.
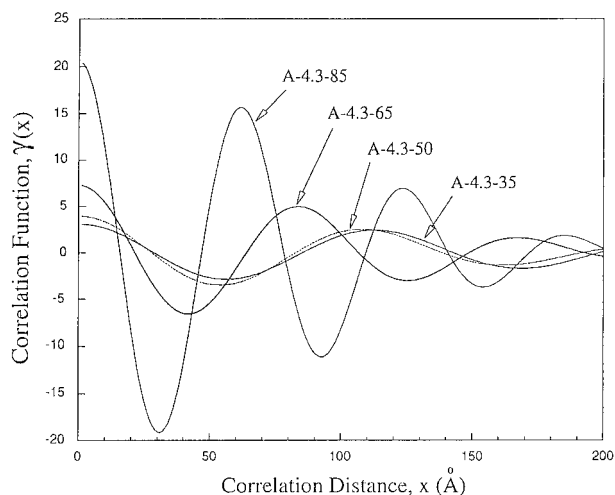
Figure 5 Correlation functions obtained from SAXS measurements for H-networks.
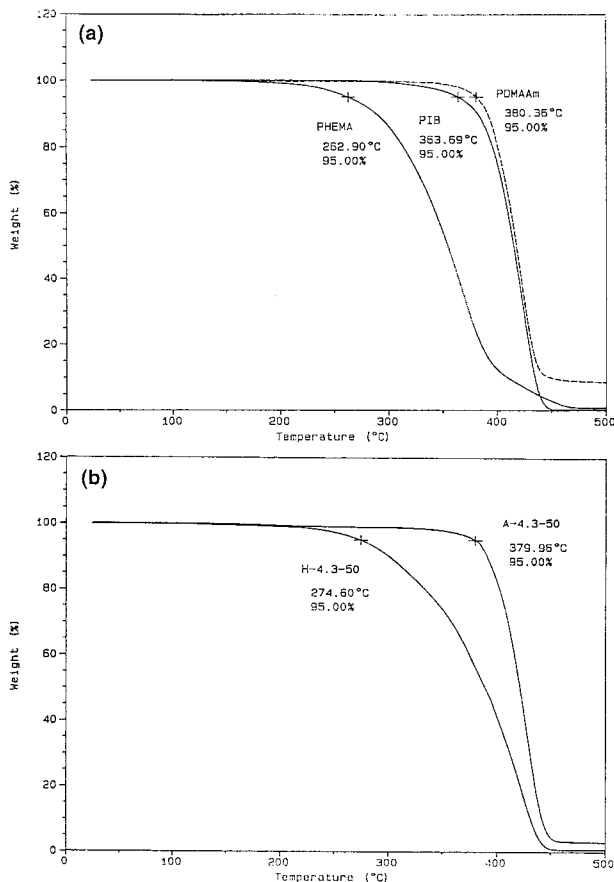
Figure 6 Thermogravimetric analysis of (a) homopolymer networks (PHEMA, PIB, and PDMAAm), and (b) H-4.3-50 and A-4.3-50. The location of the "+" mark indicates a temperature of 5% of weight loss. Heating rate was 10°C/min in air.

paring the value for n-heptane-swollen H-4.3-50 with that for water-swollen H-4.3-35; the value was higher for heptane-swollen H-4.3-50 than for water-swollen H-4.3-35, where the extent of swelling is higher for the latter. Apparently, the hydrophilic component swells in water while the flexible hydrophobic component collapses, resulting in a small increase in the total volume of the swollen network; in n-heptane, the hydrophobic component swells, while the stiff hydrophilic component does not collapse, which leads to a considerable increase in the total volume.

Thermal Stability

The thermal degradation of homopolymers and amphiphilic networks was investigated by a thermogravimetric analyzer. Degradation temperatures were compared at the same conditions: at temperatures of 5% weight loss as indicated by the "+" mark in Figure 6. PDMAAm networks

exhibited higher thermal stability than the other homopolymer and H- and A-networks, although the PIB network showed quite a high degradation temperature. The PHEMA network showed the lowest thermal stability, therefore it was not too surprising to find that the degradation temperature of H-4.3-50 was considerably lower than that of A-4.3-50; thermal degradation of H-networks, however, will not be a problem for biomedical applications since its degradation temperature is still sufficiently high.

Dynamic Mechanical Properties

Dynamic mechanical analysis is often used to investigate not only dynamic viscoelastic properties but also transition temperatures (i.e., α-, β-, γ-transitions, etc.) which cannot be found by calorimetric methods. Generally, the T_g observed by DMTA is higher than that by DSC, and DMTA is more sensitive to heating rate and frequency than DSC; the higher the heating rate and frequency the higher the T_g. Hence, DMTA is commonly used to study transitions, and not to determine the absolute T_g, which is generally obtained by quasi-static methods like DSC. The transitions may also provide clues in regard to miscibility.

Figures 7 and 8 show the loss tangent (tan δ) and storage modulus (G') as a function of temperature for H- and A-networks, respectively. The transitions were sharper in the tan δ than in the G' traces; hence, tan δ rather than G' traces were used to discuss the transitions. In the tan δ traces, the peak at the lowest temperature is the T_g of PIB, and the one at the next lowest temperature represents that of the hydrophilic component. These T_g could easily be identified by referring to the DSC traces shown in Figure 9. The DSC traces could not yield sufficiently distinct transitions, particularly with a component present at a relatively low concentration. In both H- and A-networks, the T_g of PIB and those of the hydrophilic components shifted toward each other with increasing PIB content. This effect probably arises because the two immiscible components are held together by the PIB crosslinker, particularly when the PIB concentration is high. The DMTA data which suggest that the higher the PIB content the less the phases are separated, are in good agreement with the SAXS data, which show that average interdomain spacings decrease with increasing PIB content.

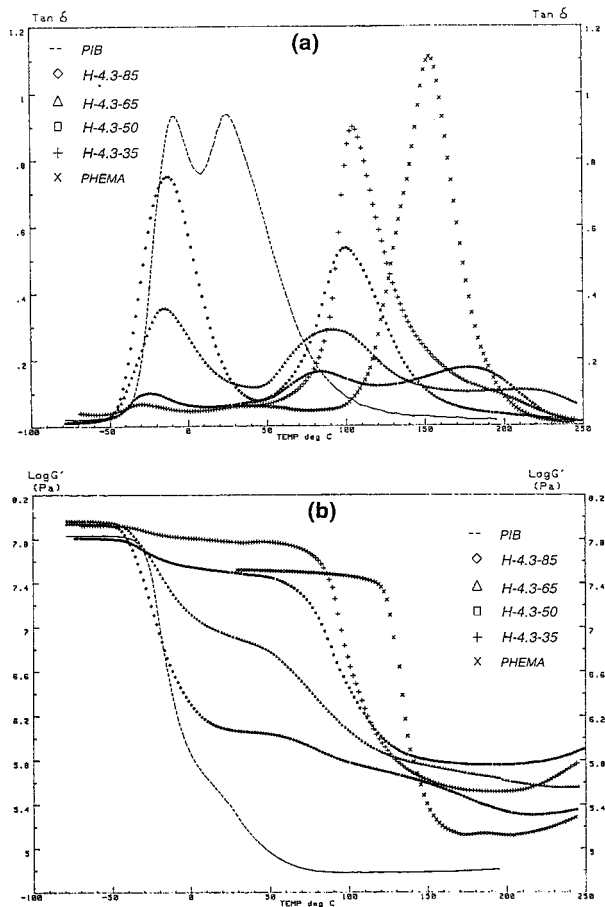The tan δ traces of some samples, for example, H-4.3-85, H-4.3-65, A-4.3-85, A-4.3-65, A-4.3-50,

Figure 7 Dynamic mechanical properties of various compositions H-networks; (a) loss tangent (tan δ); (b) storage modulus; 4°C/min heating rate and 1 Hz frequency.

and A-4.3-35, exhibited a peak above the T_g of the hydrophilic and hydrophobic components. This transition is probably the so-called "liquid–liquid transition" (T_{ll}),[21–41] although according to Hedvat[27] the rubbery-viscous transition (T_r) may be a more appropriate label. A strong relaxation above the T_g in PIB was first observed by dynamic mechanical analysis,[42] but was not assigned to T_{ll} at that time. Although there has been a lot of controversy about the existence of $T_{ll}(>T_g)$,[43–51] T_{ll} is now considered a molecular level transition-relaxation associated with the thermal disruption of segment–segment contacts.[22,23] Intermolecular segment–segment interactions produce a three-dimensional mobile physical network that "melts" at T_{ll}.[23] This segmental melting concept (or phase dualism mechanism),[52] of the several proposed molecular interpretations for the origin of T_{ll}, seems most in accord with all known facts about

T_{ll}.[22] T_{ll} has been observed in many amorphous polymers such as PIB,[38] polystyrene,[28,33,34,37] poly-(methyl methacrylate),[35,36] etc., and copolymers such as styrene–butadiene diblock copolymer,[32] styrene–butadiene–styrene triblock copolymer,[32] styrene–ethylacrylate random copolymer,[53] etc.

The origin of T_{ll} in the amphiphilic networks is most probably due to PIB chains. PIB tends to show relatively strong T_{ll} (due to chain stiffness and the stereoregularity of the polymer backbone),[22,23,38,41] and crosslinked PIB exhibits $T_{ll}(>T_g)$ (Fig. 10). Hydrophilic homopolymer networks (i.e., PHEMA and PDMAAm) do not show T_{ll}. Since crosslinking reduces the intensity of the T_{ll} transition and since only lightly crosslinked networks can show T_{ll},[23,25,38] the existence of a distinct T_{ll} in the amphiphilic networks suggests that a considerable number of PIB chains did not crosslink and may exist as dangling branches.
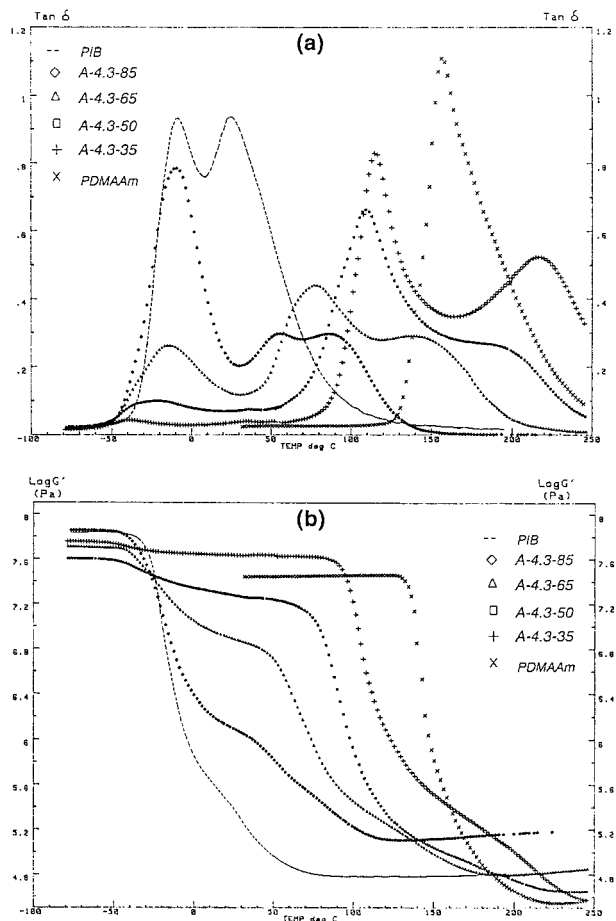

Figure 8 Dynamic mechanical properties of various compositions A-networks; (a) loss tangent (tan δ); (b) storage modulus; 4°C/min heating rate and 1 Hz frequency.
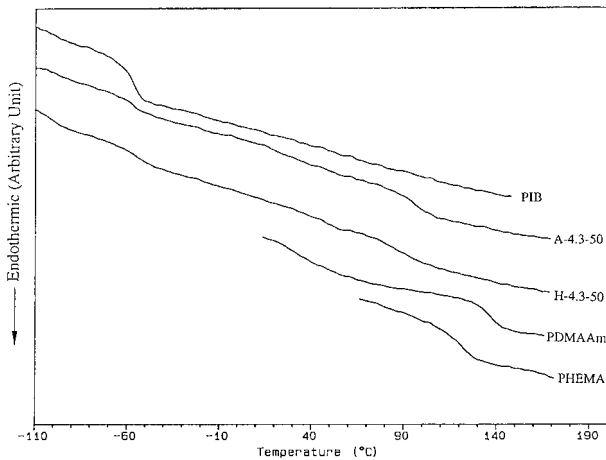
Figure 9 DSC thermograms of homopolymer and amphiphilic networks; heating rate was 10°C/min.

Figure 11 DSC thermogram of A-4.3-35; heating rate was 10°C/min.

These dangling chains, each of which will show random coil behavior, may form intermolecular segment–segment contacts that will disrupt at T_{ll}. When the T_{ll} transition for the amphiphilic networks is assumed to arise from the strong segment–segment interactions (or contacts) among the PIB dangling chains, the interactions might be particularly stronger due to the polar chain ends (methacrylate) of the PIB.

Dangling chains may form untrapped entanglements, the rearrangement or slippage of which occurs at T_{ll}.[38] However, our networks cannot contain entangled PIB chains because the $\bar{M}_n$ of PIB used in the synthesis was much lower than the entanglement molecular weight (M_e) of PIB (i.e., < 15,200 g/mol).[54] At the same PIB content, H-networks showed weaker but higher T_{ll} than A-
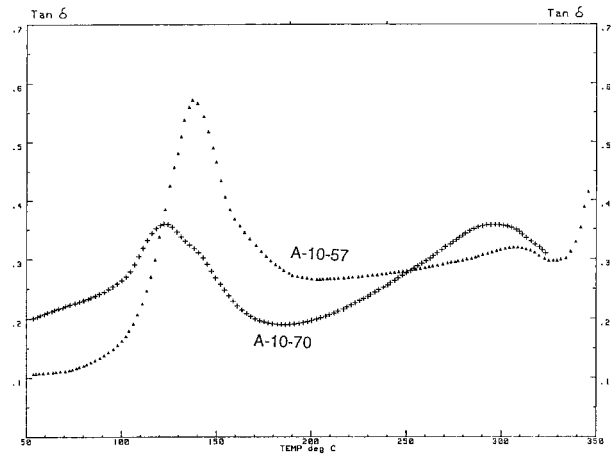
networks, and gradually the T_{ll} disappeared with increasing hydrophilic component. This suggests that the crosslink density of H-networks is higher than that of A-networks because, just as in the case of T_g, crosslinking raises the T_{ll} and decreases its intensity. As shown for both A- and H-networks, the T_{ll} is higher with higher hydrophilic content because the stiff and hard hydrophilic component acts as a physical crosslink. The hydrophilic component in the amphiphilic networks also affects the value of T_{ll}. It has been accepted that

$$T_{ll}(K) = (1.20 \pm 0.05)T_g(K)$$

for most polymers.[22–26,41] T_{ll}/T_g was 1.12 for the PIB network, but was much higher for networks of high hydrophilic content; for example, T_{ll}/T_g
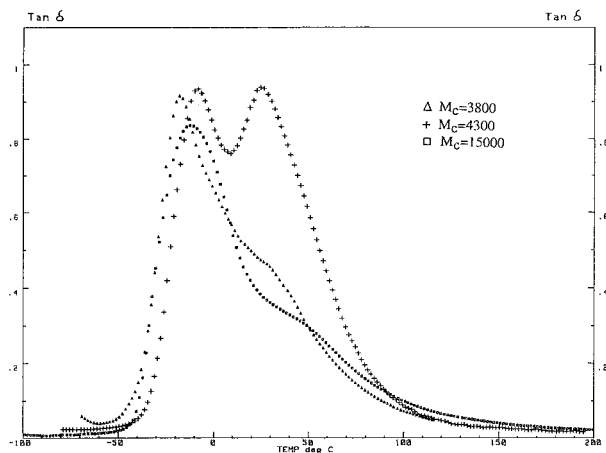

Figure 10 Loss tangent curves of various M_c PIB; 4°C/min heating rate and 1 Hz frequency.
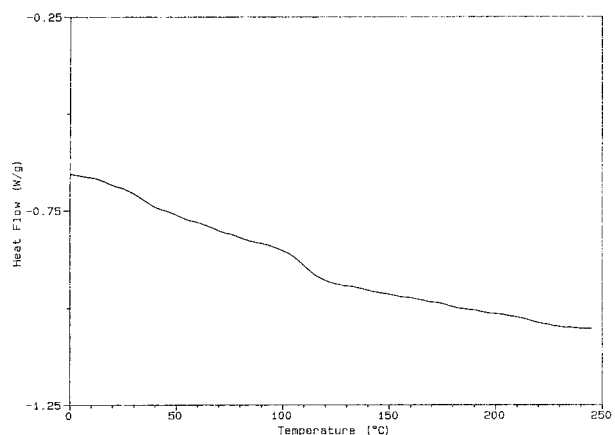

Figure 12 Loss tangent curves of A-10-57 and A-10-70; 4°C/min heating rate and 1 Hz frequency.
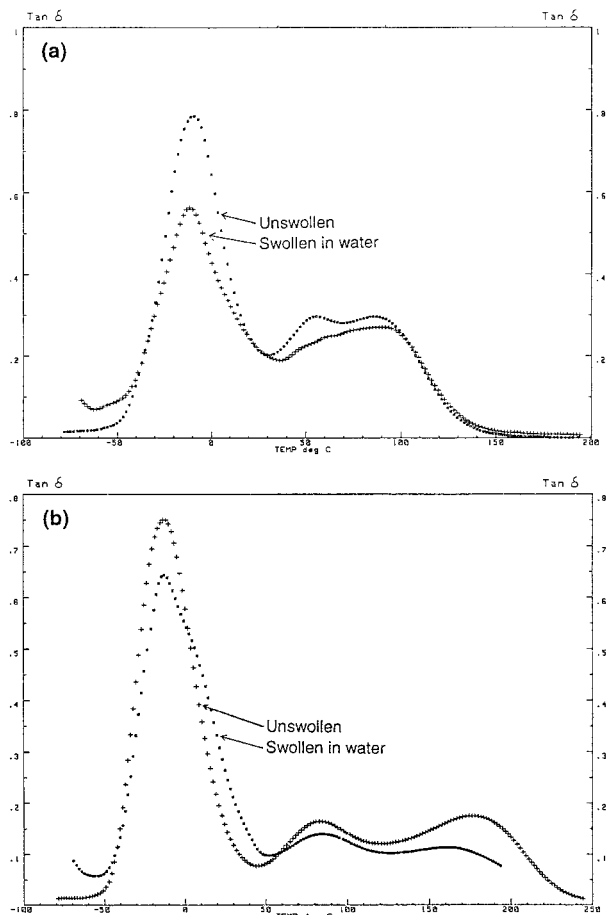
Figure 13 The effect of water-swelling on loss tangent curves of (a) A-4.3-85 and (b) H-4.3-85; 4°C/min heating rate and 1 Hz frequency.

= 2.10 for A-4.3-35. Therefore, the above equation can not be applied to amphiphilic networks.

As shown by Figure 11, T_{ll} is also present in A-networks with higher $\bar{M}_n$ of PIB (i.e., A-10-57 and A-10-70) but appears at ∼ 300°C, indicating that T_{ll} increases with $\bar{M}_n$.[21–23,26,31] The tan δ data ≳ 320°C should be disregarded because of significant thermal degradation (see Fig. 6).

T_{ll} could not be detected by DSC. For example, A-4.3-35, whose T_{ll} in the tan δ trace was most conspicuous at ∼ 217°C, did not show this transition by DSC (Fig. 12); if it exists, an endothermic event should appear at 205°C or below in the DSC trace because the transition temperature in DSC is lower than by DMTA. There are many possible reasons why T_{ll} could not be detected by DSC: since T_{ll} is an endothermic event and is generally a weaker transition than T_g, other endothermic reactions, such as depolymerization or evaporation of volatiles, may obscure DSC analysis.[23] An

exothermic event, such as oxidation,[55] may also weaken or destroy T_{ll}.[23]

Figure 13 shows the effect of water-swelling on the transitions of A-4.3-85 and H-4.3-85. The sizes of both the T_g and T_{ll} peaks were reduced by swelling, implying that a diluent (H_2O) can reduce the damping at these transitions. Swelling did not affect the T_g of the hydrophobic or hydrophilic components of the A- and H-networks, while the T_{ll} of H-4.3-85 was reduced.

REFERENCES

1. J. P. Kennedy, U.S. Pat. 4,942,204 (1990).
2. D. Chen, J. P. Kennedy, and A. J. Allen, *J. Macromol. Sci., Chem.,* **A25,** 389 (1988).
3. B. Iván, J. P. Kennedy, and P. W. Mackey, in *Polymeric Drugs and Drug Delivery Systems,* R. L. Dunn and R. M. Ottenbrite, Eds., ACS Symposium Series 469, Washington, DC, 1990, p. 194.
4. B. Iván, J. P. Kennedy, and P. W. Mackey, in *Polymeric Drugs and Drug Delivery Systems,* R. L. Dunn and R. M. Ottenbrite, Eds., ACS Symposium Series 469, Washington, DC, 1990, p. 204.
5. P. W. Mackey, Ph.D. dissertation, The University of Akron, 1991.
6. B. Keszler, J. P. Kennedy, and P. W. Mackey, *J. Contr. Rel.,* **25,** 115 (1993).
7. D. Chen, J. P. Kennedy, M. M. Kory, and D. L. Ely, *J. Biomed. Mater. Res.,* **23,** 1327 (1989).
8. B. Keszler, J. P. Kennedy, N. P. Ziats, M. R. Brunstedt, S. Stack, J. K. Yun, and J. M. Anderson, *Polym. Bull.,* **29,** 681 (1992).
9. D. Park, V. Galiatsatos, B. Keszler, J. P. Kennedy, and B. D. Ratner, *Polym. Prepr., Am. Chem. Soc., Div. Polym. Chem.,* **34,** 62 (1993).
10. D. Park, B. Keszler, V. Galiatsatos, J. P. Kennedy, and B. D. Ratner, *Macromolecules,* **28,** 2595 (1995).
11. B. Keszler and J. P. Kennedy, *J. Polym. Sci., Part A: Polym. Chem.,* to appear.
12. D. J. Lyman and K. Knutson, in *Biomedical Polymers; Polymeric Materials and Pharmaceuticals for Biomedical Use,* E. P. Goldberg and A. Nakajima, Eds., Academic Press, New York, 1980, p. 23.
13. Y. Sakurai, T. Akaike, K. Kataoka, and T. Okano, in *Biomedical Polymers; Polymeric Materials and Pharmaceuticals for Biomedical Use,* E. P. Goldberg and A. Nakajima, Eds., Academic Press, New York, 1980, p. 335.
14. T. Okano, Y. Sakurai, and K. Kataoka, *Eur. Polym. J.,* **19,** 929 (1983).
15. M. Shimada, M. Miyahara, H. Tahara, I. Shino-

hara, T. Okano, K. Kataoka, and Y. Sakurai, *Polym. J.,* **15,** 649 (1983).

16. T. Okano, S. Nishiyama, I. Shinohara, T. Akaike, Y. Sakurai, K. Kataoka, and T. Tsuruta, *J. Biomed. Mater. Res.,* **15,** 393 (1981).

17. T. Okano, M. Uruno, N. Sugiyama, M. Shimada, I. Shinohara, K. Kataoka, and Y. Sakurai, *J. Biomed. Mater. Res.,* **20,** 1035 (1981).

18. D. Tyagi, J. E. McGrath, and G. L. Wilkes, *Polym. Eng. Sci.,* **26,** 1371 (1986).

19. C. U. Yu and J. E. Mark, *Macromolecules,* **7,** 229 (1974).

20. ASTM Standard, Designation: D 2240-86.

21. R. F. Boyer, in *Computational Modeling of Polymers,* J. Bicerano, Ed., Marcel Dekker, New York, 1992, p. 1.

22. R. F. Boyer, in *Encyclopedia of Polymer Science Engineering,* Vol. 17, J. Kroschwitz, Ed., Wiley, New York, 1989, p. 23.

23. R. F. Boyer, in *Polymer Yearbook,* Vol. 2, R. A. Pethrick, Ed., Harwood Academic, New York, 1985, p. 233.

24. R. F. Boyer, in *Encyclopedia of Polymer Science Technology,* Vol. 2, Suppl., N. M. Bikales, Ed., Wiley, New York, 1977, p. 765.

25. R. F. Boyer, *Rubber Chem. Technol.,* **36,** 1303 (1963).

26. R. F. Boyer, *J. Macromol. Sci., Phys.,* **B18,** 461 (1980).

27. S. Hedvat, *Polymer,* **22,** 774 (1981).

28. S. J. Stadnicki, J. K. Gilham, and R. F. Boyer, *J. Appl. Polym. Sci.,* **20,** 1245 (1976).

29. J. K. Gilham, J. A. Benci, and R. F. Boyer, *Polym. Eng. Sci.,* **16,** 357 (1976).

30. J. Heijboer, *Polym. Eng. Sci.,* **19,** 664 (1979).

31. R. F. Boyer, *Polym. Eng. Sci.,* **19,** 732 (1979).

32. J. K. Gilham, *Polym. Eng. Sci.,* **19,** 749 (1979).

33. J. B. Enns, R. F. Boyer, H. Ishida, and J. L. Koenig, *Polym. Eng. Sci.,* **19,** 756 (1979).

34. R. F. Boyer, *J. Appl. Polym. Sci.,* **33,** 955 (1987).

35. A. Gourari, M. Bendaoud, C. Lacabanne, and R. F. Boyer, *J. Polym. Sci., Polym. Phys.,* **23,** 889 (1985).

36. L. R. Denny, R. F. Boyer, and H. Elias, *J. Macromol. Sci., Phys.,* **B25,** 227 (1986).

37. J. K. Gilham and R. F. Boyer, *J. Macromol. Sci., Phys.,* **B13,** 497 (1977).

38. R. F. Boyer and J. B. Enns, *J. Appl. Polym. Sci.,* **32,** 4075 (1986).

39. S. E. Keinath and R. F. Boyer, *J. Appl. Polym. Sci.,* **28,** 2105 (1983).

40. J. F. Sanders and J. D. Ferry, *Macromolecules,* **7,** 681 (1974).

41. R. F. Boyer, in *Order in the Amorphous "State" of Polymers;* S. E. Keinath, R. L. Miller, and J. K. Reike, Eds., Plenum Press, New York, 1987, p. 135.

42. E. B. Fitzgerald, L. D. Gradine, and J. D. Ferry, *J. Appl. Phys.,* **24,** 650 (1953).

43. L. Nielsen, *Polym. Eng. Sci.,* **17,** 713 (1977).

44. R. M. Neumann, G. A. Senich, and W. J. Macnight, *Polym. Eng. Sci.,* **18,** 624 (1978).

45. R. M. Neumann and W. J. Macnight, *J. Polym. Sci., Polym. Phys. Ed.,* **19,** 369 (1981).

46. D. J. Plazek, *J. Polym. Sci., Polym. Phys. Ed.,* **20,** 1533 (1982).

47. D. J. Plazek and G. F. Gu, *J. Polym. Sci., Polym. Phys. Ed.,* **20,** 1551 (1982).

48. J. Chen, C. Kow, L. J. Fetters, and D. J. Plazek, *J. Polym. Sci., Polym. Phys. Ed.,* **20,** 1565 (1982).

49. S. J. Orbon and D. J. Plazek, *J. Polym. Sci., Polym. Phys. Ed.,* **20,** 1575 (1982).

50. R. F. Boyer, *J. Polym. Sci., Polym. Phys. Ed.,* **23,** 21 (1985).

51. R. F. Boyer, *J. Polym. Sci., Polym. Phys. Ed.,* **23,** 1 (1985).

52. A. M. Lobanov, S. Ya. Frenkel, *Polym. Sci., USSR,* **22,** 1150 (1980).

53. P. L. Kumler, G. A. Machajewski, J. J. Fitzgerald, L. R. Denny, S. E. Keinath, and R. F. Boyer, *Macromolecules,* **20,** 1060 (1987).

54. W. W. Graessley and S. F. Edwards, *Polymer,* **22,** 1329 (1982).

55. L. R. Denny, K. M. Penichella, and R. F. Boyer, *J. Polym. Sci., Plym. Symp.,* **71,** 39 (1984).